



Original Articles

Metabolic targeting synergizes with MAPK inhibition and delays drug resistance in melanoma



Christina Brummer^a, Stephanie Faerber^{a,b}, Christina Bruss^a, Christian Blank^c, Ruben Lacroix^c, Sebastian Haferkamp^d, Wolfgang Herr^a, Marina Kreuz^{a,b}, Kathrin Renner^{a,b,*}

^a Department of Internal Medicine III, University Hospital of Regensburg, Regensburg, Germany

^b Regensburg Center for Interventional Immunology (RCI), Regensburg, Germany

^c Department of Medical Oncology and Division of Molecular Oncology & Immunology, The Netherlands Cancer Institute, Amsterdam, the Netherlands

^d Department of Dermatology, University Hospital of Regensburg, Regensburg, Germany

ARTICLE INFO

Keywords:

BRAF
Vemurafenib
Glycolysis
MITF
Diclofenac
NSAID

ABSTRACT

Tumors, including melanomas, frequently show an accelerated glucose metabolism. Mutations in the v-Raf murine sarcoma viral oncogene homolog B (BRAF), detected in about 50% of all melanomas, result in further enhancement of glycolysis. Therefore anti-metabolic substances might enhance the impact of RAF inhibitors. We have identified the two non-steroidal anti-inflammatory drugs (NSAIDs) diclofenac and lumiracoxib being able to restrict energy metabolism in human melanoma cells by targeting lactate release and oxidative phosphorylation (OXPHOS). In combination with the RAF inhibitor vemurafenib strong synergism was observed: Diclofenac as well as lumiracoxib increased the anti-glycolytic impact of vemurafenib and prevented RAF-inhibitor induced metabolic reprogramming towards OXPHOS. Consequently, both NSAIDs sensitized melanoma cells to vemurafenib triggered proliferation arrest and enhanced the anti-tumor effect of RAF inhibitors from cytostatic to cytotoxic. Furthermore the addition of NSAIDs delayed the onset of RAF inhibitor resistance, most likely by counteracting the upregulation of MITF. Our data suggest that selected NSAIDs could be a promising combination partner for MAPK pathway inhibitors for the treatment of BRAF^{V600E} mutated melanomas.

1. Introduction

The approval of RAF inhibitors has revolutionized the treatment of late-stage melanoma, the most aggressive form of skin cancer, several years ago [1]. BRAF inhibitors such as vemurafenib and dabrafenib selectively target cells harboring oncogenic BRAF mutations accounting for MAPK pathway hyper-activation in approximately 50% of all melanomas [2]. However, most patients show promising initial response, but develop disease progression within a few months due to acquisition of drug resistance [3]. As single treatment does not result in durable disease control, standard-of-care protocols for BRAF mutated melanoma have shifted from mono- towards combination therapy [4,5]. Combined treatment protocols, e.g. of BRAF and MEK inhibitors, reveal significantly higher response rates and progression free survival (PFS). However, long-term benefit is often limited to a small fraction of patients [6,7]. Thus there is still a strong need for identifying additional

combinatory treatment options.

Recently, targeting cancer metabolism has been discussed as a promising strategy in melanoma treatment [8–10]. Metabolic reprogramming towards enhanced glycolysis, commonly known as the “Warburg effect” [11], is a recognized hallmark of cancer [12] and has been shown for many different tumor types, including malignant melanoma [13–15]. In order to fulfil their demand for biomolecule intermediates and energy, tumor cells display an accelerated metabolic activity and metabolize glucose mainly to lactate instead of using it for ATP production via oxidative phosphorylation. The BRAF^{V600E} mutation has been associated with this highly glycolytic phenotype [16], indicating that V600E mutated melanoma tumors depend even more on glucose than BRAF wildtype counterparts [17]. Indeed, Parmenter et al. confirmed that the BRAF oncogene upregulates a network of glycolysis triggering transcription factors downstream the C-MYC/HIF1 α axis [18]. Moreover Haq and colleagues have shown the Warburg

Abbreviations: CI, combination index; diclo, diclofenac; FA, fraction affected; lumira, lumiracoxib; MITF, microphthalmia-associated transcription factor; mtATPi, mitochondrial ATP-Synthase inhibitor; MAPK, mitogen-activated protein kinase; MCT, monocarboxylate transporter; NSAID, non-steroidal anti-inflammatory drug; OXPHOS, oxidative phosphorylation; vemura, vemurafenib

* Corresponding author. Department of Internal Medicine III, University Hospital of Regensburg, Franz-Josef-Strauß-Allee 11, D-93053, Regensburg, Germany.

E-mail address: kathrin.renner-sattler@ukr.de (K. Renner).

<https://doi.org/10.1016/j.canlet.2018.11.018>

Received 26 September 2018; Received in revised form 8 November 2018; Accepted 9 November 2018

0304-3835/© 2018 Elsevier B.V. All rights reserved.

phenotype to be further promoted by BRAF-induced attenuation of central regulators of oxidative phosphorylation (OXPHOS) such as the microphthalmia-associated transcription factor (MITF) [19,20]. Vice versa, RAF inhibitor treatment suppresses glucose metabolism [21] and renders BRAF^{V600E} mutated melanoma cells addicted to respiration [19,22]. Therefore the combination of RAF inhibitors and agents targeting OXPHOS has been discussed as a highly promising therapeutic strategy to enhance impact of MAPK pathway inhibition [23,24] and overcome drug resistance [25,26].

However, metabolic flexibility might limit the efficacy of one-armed anti-metabolic approaches in melanoma [27]. Previously our group has shown that the nonsteroidal anti-inflammatory drug (NSAID) diclofenac diminishes lactate secretion and affects oxidative phosphorylation in a variety of cancer cell lines [28]. In this study we demonstrate that diclofenac and also lumiracoxib, another NSAID displaying a high structural similarity to diclofenac, reveal a comparable dual anti-metabolic impact on BRAF^{V600E} mutated melanoma cells. The combination of the RAF inhibitor vemurafenib with either NSAID restricts metabolic reprogramming and efficiently starves the cells resulting in a highly synergistic effect on proliferation as well as cell death induction. Furthermore low-dose NSAID treatment reduces MITF expression and delays onset of RAF inhibitor resistance in a long-term treatment approach.

2. Materials and methods

2.1. Cells and cell culture

BRAF^{V600E} mutated human melanoma cell lines (MelIM, M14, SK-Mel-28) were cultured in RPMI 1640 (Gibco) with 10% FCS and 2 mM instabile L-glutamine (both from PAN Biotech) at 5% CO₂ and 37 °C. Cells were passaged and reseeded (0.05 × 10⁶ cells/ml) every 72–96 h at around 80% confluency. MelIM was obtained from Prof. Judith Johnson (formerly Institute of Immunology, LMU Munich, Germany) in 1993 and has been characterized before [29]. SK-Mel-28 and M14 were kindly provided by Dr. Sebastian Haferkamp (Department of Dermatology, University Hospital Regensburg, Germany) [30].

2.2. Chemicals

Vemurafenib (Selleckchem, S1267, stock concentration 1 mM) was dissolved in ethanol (Roth). Diclofenac (Fagron, 135796, stock concentration 8 mM) was dissolved in RPMI and lumiracoxib (Selleckchem, S2903, stock concentration 200 mM) in DMSO (Honeywell Riedel-de Haen). Oligomycin (Sigma-Aldrich, O4876, stock concentration 5 mM) was dissolved in ethanol.

2.3. Cell number, doubling time and viability determination

For proliferation and viability analysis cells were seeded into flat-bottom 6-well-plates (0.15 × 10⁶ cells/well) with or without indicated concentrations of drugs. Carrier controls were included in every treatment set and had no significant impact on determined parameters compared to untreated controls, unless otherwise indicated. After the indicated time of incubation cells were harvested with trypsin (Gibco) and counted with a CASY TT Cell Counter and Analyzer (OLS). Results have been normalized to the initial number of cells seeded and given as percent of the untreated control.

To distinguish between viable and apoptotic cells, double-staining with FITC labeled Annexin-V and 7-Aminoactinomycin (7-AAD) (both from BD Biosciences) was performed. Subsequent flow cytometry was carried out on a FACS Calibur (BD Biosciences) using CellQuestPro for data acquisition and FlowJo Software for data analysis. Annexin-V positive, but 7-AAD negative cells were classified as early apoptotic and double-positive cells as late apoptotic, while double negative cells were regarded as viable. Doubling time T_d of cells was calculated according

to the following formula [31]:

$$(eq. 1) T_d = \frac{\text{duration} * \log(2)}{\log(\text{final cells}) - \log(\text{initial cells})}$$

2.4. Metabolic restriction

For nutrient starvation cells were incubated in 6-well-plates (0.15 × 10⁶ cells/well) for 72 h under the following conditions: Glucose metabolism was deprived by using glucose-free RPMI medium (Sigma Aldrich). Mitochondrial ATP production was inhibited by addition of the ATP-synthase inhibitor oligomycin (final concentration 5 μM).

2.5. Lactate measurement in cell culture supernatants

For metabolite quantification cells were cultured in flat-bottom 6-well-plates (0.15 × 10⁶ cells/well) for 72 h. After the indicated time lactate levels in cell culture supernatants were measured enzymatically using commercially available reagents from Roche and an ADVIA 1650 (Bayer). For analysis of metabolite consumption or release rates (CORE) measured lactate concentrations were normalized to kinetics of tumor cell growth according to the method of Jain et al. [32].

2.6. Oxygen consumption and staining for mitochondrial content

To analyze mitochondrial content cells were cultivated in 6-well-plates for 72 h, harvested and stained with MitoTracker Green FM (Invitrogen) for 2 h. To block export of MitoTracker Green via multi-drug resistance transporters cyclosporine A (Sandimmun®, Novartis) was added. Stained cells were analyzed in terms of mitochondrial content by flow cytometry. Unstained cells were used to determine auto-fluorescence.

Respiration was quantified using the PreSens technology (PreSens Precision Sensing GmbH) that allows non-invasive online monitoring of oxygen under standard cell culture conditions. Therefore cells were seeded in specialized 24-well-plates (Oxodish® OD24) at a density of 0.2 × 10⁶/ml and incubated for the indicated period of time.

2.7. Western blotting

For protein analysis cells were seeded into flat-bottom 6-well-plates for 24 h (2.5 × 10⁶ cells/well). Cell lysates were prepared with RIPA-buffer and samples were subjected to western blotting on a denaturing 12% acrylamide gel. Membranes were tested against a MITF antibody from Santa Cruz (sc-56725). β-actin (Sigma) was used as a loading control.

2.8. Drug interaction analyses

For drug interaction analyses combination indices (CI) were determined according to the algorithm of Chou Talalaly using CompuSyn [33]. Being an applied method in anti-cancer research, CI values represent a computerized simulation system for the analysis of drug interactions regardless of their mechanism of action. CI < 0.9 indicates synergism, 1.1 < CI < 0.9 additivism and CI > 1.1 antagonism of the analyzed drugs. As recommended combinatorial concentrations were chosen in a fixed constant ratio approximately according to the IC₅₀ ratio (eq. 2) of the single drugs [34]:

$$(eq. 2) \frac{c(\text{BRAFi})}{c(\text{NSAID})} \cong \frac{IC_{50}(\text{BRAFi})}{IC_{50}(\text{NSAID})} \cong \frac{1}{1000}$$

For drug interaction analysis fractions affected (FA) for growth inhibition (eq. 3) and cell death induction (eq. 4) were determined as shown by the following formulas and entered into the CompuSyn software:

$$(eq. 3) FA_{\text{growth inhibition}} = 1 - \frac{[\text{proliferation}]_{\text{treated}}}{[\text{proliferation}]_{\text{control}}}$$

$$(eq. 4) FA_{\text{cell death induction}} = 1 - \frac{[\text{viability}]_{\text{treated}}}{[\text{viability}]_{\text{control}}}$$

Methods of proliferation and cell viability determination have been outlined above. As previously described [34], values higher than 100% (FA < 0) or less than 0% (FA > 1) were set as 100% or 0%.

2.9. Statistical analysis and data plotting

Statistical analysis was performed using Graph Pad Prism 7. Results represent the mean of a minimum of three independent experiments (n ≥ 3) shown with the standard error of the mean (SEM). Unless otherwise indicated, treatment groups were compared via one-way ANOVA and posthoc Dunnett's multiple comparisons test. Significant differences are shown by * (*p < 0.05, **p < 0.01, ***p < 0.001).

3. Results

3.1. BRAF^{V600E} mutated melanoma cells display a high metabolic flexibility

BRAF-mutated melanomas are known to exhibit a high glycolytic activity [13]. To analyze dependency on metabolic pathways in more detail, a panel of BRAF^{V600E} mutated human melanoma cell lines (MelIM, SK-Mel-28, M14) was cultured in glucose free medium (0-Glc), treated with the mitochondrial ATP synthase inhibitor (mtATPi) oligomycin or the combination of both (Fig. 1A and Fig. S1A). Interestingly, restriction of either glucose metabolism or mitochondrial ATP (mtATP) production only led to a 40–60% growth inhibition each. However, when both pathways were inhibited, proliferation was completely blocked (Fig. 1A) and, moreover, cell viability was reduced (Fig. S1B). These data indicate that restriction of a single energy providing pathway is not sufficient to completely arrest proliferation or affect viability of the BRAF^{V600E} mutated melanoma cell lines investigated. Hence, we hypothesized that metabolic restriction might be compensated by alternative pathways and measured lactate levels in cell culture supernatants (Fig. S1C). Increased lactate release rates under oligomycin treatment confirmed counteraction of OXPHOS inhibition by enhanced glucose metabolism in all three cell lines (Fig. 1B). Vice versa, under glucose deprivation a slight upregulation of mitochondrial content was observed (data not shown).

These results suggest that anti-metabolic agents represent a promising treatment option for BRAF^{V600E} mutated melanoma cells, but high metabolic flexibility limits efficiency of drugs targeting only one single energy providing pathway.

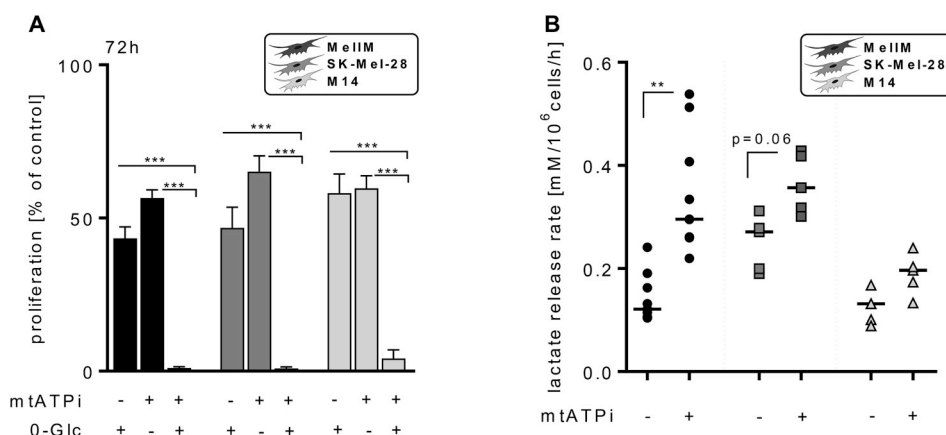


Fig. 1. Metabolic profile of BRAF^{V600E} mutated melanoma cell lines. (A) Proliferation of MelIM, SK-Mel-28 and M14 cells either in standard growth medium ± the mitochondrial ATP synthase inhibitor oligomycin (mtATPi) or in glucose-free medium (0-Glc) ± mtATPi. Cell numbers were counted by the CASY system. Results are normalized to untreated controls (mean ± SEM, ordinary one-way ANOVA and post-hoc Tukey's multiple comparisons test ***p < 0.001; MelIM: n = 14 for 0-Glc and n = 11 for mtATPi, independent experiments four times performed in at least duplicates; n = 6 for 0-Glc + mtATPi; SK-Mel-28: n = 9; M14: n = 10 independent experiments for 0-Glc or mtATPi, three times performed in at least duplicates; n = 3 for 0-Glc + mtATPi). (B) Lactate release rates of melanoma cell lines incubated with or without mtATPi. Lactate levels were measured in cell culture supernatants after 72 h, corrected for basal medium values and normalized for proliferation (Wilcoxon matched-pairs signed rank test; **p < 0.01).

3.2. Selected NSAIDs affect melanoma cell lines by metabolic restriction

Previously, our group has shown that the NSAID diclofenac is able to block lactate secretion and proliferation in a variety of cancer cell lines including the human melanoma cell line MelIM [28]. To test whether these results are reproducible in BRAF^{V600E} mutated melanoma cells *per se*, proliferation and metabolic activity of MelIM, SK-Mel-28 and M14 was monitored under increasing concentrations of diclofenac. As expected, significant growth inhibition was observed in all cell lines analyzed (Fig. 2A). Comparable results were also obtained with lumiracoxib (Fig. 2A), a NSAID displaying a high structural similarity to diclofenac. Interestingly concentrations higher than 0.1 mM diclofenac also triggered cell death (Fig. 2B). For lumiracoxib concentrations of 0.4 mM were needed to induce apoptosis *in vitro* (Fig. 2B and data not shown).

Next, the metabolic impact of both NSAIDs was analyzed. Diclofenac as well as lumiracoxib led to diminished lactate release rates at concentrations as low as 0.05 μM in MelIM (Fig. 2C), SK-Mel-28 and M14 (not shown). In line with lower IC₅₀ values, diclofenac had a slightly stronger impact on lactate release rates than lumiracoxib at equivalent concentrations. To evaluate the kinetics of NSAID-induced glycolytic inhibition and proliferation arrest in more detail, lactate secretion and cell number were monitored in parallel over 48 h (Fig. S2). While lactate production was diminished already after 12 h of diclofenac treatment by more than 50% (Fig. S2A), significant cell number reduction was not observed within 48 h (Fig. S2B). These results confirm that the metabolic impact of the selected NSAIDs occurs prior to proliferation arrest.

However, since glucose deprivation alone reduced proliferation only by 50% (Fig. 1A) and did not result in significant cell death induction (Fig. S1B), we assumed that glycolytic restriction alone doesn't explain the observed growth inhibitory effects under diclofenac and lumiracoxib treatment. The fact that simultaneous deprivation of glucose and mtATP induced apoptosis (Fig. S1B), led us to the hypothesis that diclofenac and lumiracoxib might not only have an impact on lactate secretion but also on mitochondrial activity. Indeed, mitochondrial content of MelIM was significantly downregulated by both NSAIDs after 72 h (Fig. 2D). Monitoring oxygen consumption further confirmed inhibition of respiration at concentrations higher than 0.05 mM diclofenac (Fig. 2E) and 0.1 mM lumiracoxib, respectively (Fig. 2F). Notably, cell number dependent effects were negligible at this time point and concentration (Fig. S2B).

In conclusion, the selected NSAIDs reveal dual anti-metabolic effects on melanoma by inhibiting both lactate secretion and mitochondrial activity and therefore represent a promising therapeutic option for metabolically highly active tumor cells.

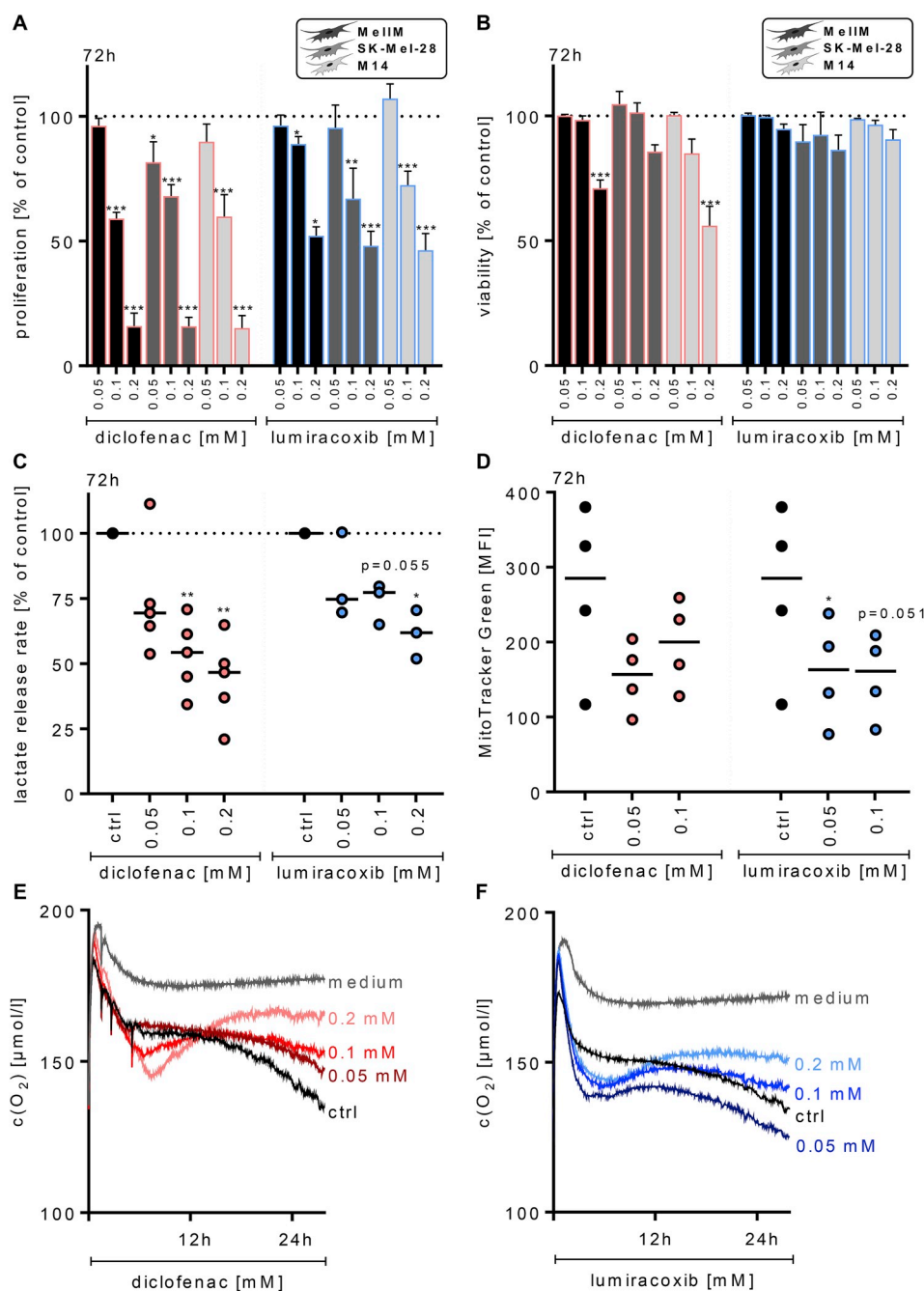


Fig. 2. Impact of the NSAIDs diclofenac and lumiracoxib on BRAF^{V600E} mutated melanoma cell lines. (A) Proliferation and (B) cell viability of MelIM, SK-Mel-28 and M14 under treatment with diclofenac or lumiracoxib (0.05–0.2 mM) for 72 h, results were normalized to respective controls. Proliferation was determined using a CASY cell counter and was corrected for the cell number seeded (mean + SEM; diclofenac: n = 5 for MelIM/SK-Mel-28 and n = 6 for M14; lumiracoxib: n = 9 for MelIM and n = 5 for SK-Mel-28/M14). Cell viability was analyzed by Annexin-V/7-AAD staining (mean + SEM; diclofenac: n = equivalent to proliferation, lumiracoxib: n = 8 for MelIM, n = 4 for SK-Mel-28, n = 5 for M14; one-way ANOVA post-hoc Dunnett's multiple comparisons test *p < 0.05, **p < 0.01, ***p < 0.001). (C) Lactate release rates and (D) mitochondrial content of MelIM cells under diclofenac or lumiracoxib treatment. Lactate levels were measured in cell culture supernatants after 72 h and corrected for basal medium values as well as proliferation kinetics. Mitochondrial content was analyzed by MitoTracker Green staining of MelIM incubated in standard growth medium ± the addition of diclofenac or lumiracoxib for 72 h. Mean fluorescence intensity (MFI) of MitoTracker Green was normalized to unstained cells (one-way ANOVA post-hoc Dunnett's multiple comparisons test *p < 0.05, **p < 0.01, ***p < 0.001). Monitoring of oxygen consumption of MelIM cells incubated in standard growth medium (control) (E) ± diclofenac or (F) ± lumiracoxib. Data were acquired with the PreSens technology under standard cell culture conditions for 24 h (mean; diclofenac: n = 7; lumiracoxib: n = 5 independent experiments, two times performed in at least duplicates). (For interpretation of the references to color in this figure legend, the reader is referred to the Web version of this article.)

3.3. Targeting metabolic reprogramming enhances the impact of RAF-inhibitors

Most BRAF^{V600E} mutated melanoma respond to BRAF inhibitors (BRAFi) such as vemurafenib. As expected, vemurafenib treatment resulted in a strong proliferation arrest in all cell lines used (Fig. 3A). However, only a slight reduction of cell viability was observed (Fig. 3B). Since the BRAF oncogene is known as a driver mutation for metabolic reprogramming, metabolic flexibility might be one mechanism of melanoma cells escaping from cell death induction under BRAF inhibition (Fig. 1 and Fig. S1). In accordance with this hypothesis, cells treated with vemurafenib displayed diminished lactate release rates up to 50% (Fig. 3C). In turn, mitochondrial content was significantly upregulated indicating a compensatory switch from

glycolysis to OXPHOS under BRAF inhibition (Fig. 3D). Indeed, monitoring oxygen consumption of MelIM cells confirmed enhanced respiration under vemurafenib treatment (Fig. 3E).

To test whether blocking metabolic plasticity could further enhance the impact of BRAF inhibitors, MelIM cells were treated with vemurafenib and the ATP synthase inhibitor oligomycin (Fig. 3F). As expected, the addition of oligomycin further increased proliferation arrest (Fig. 3F) compared to single treatment with vemurafenib (Fig. 3A). However, apoptosis induction was not increased (Fig. S3). As complete deprivation of mtATP and glucose has caused cell death (Fig. S1B), the remaining glycolytic activity might be sufficient to maintain cell viability.

Hence, dual metabolic inhibition of both glycolysis and metabolic reprogramming towards OXPHOS could be a promising strategy to enhance the impact of vemurafenib.

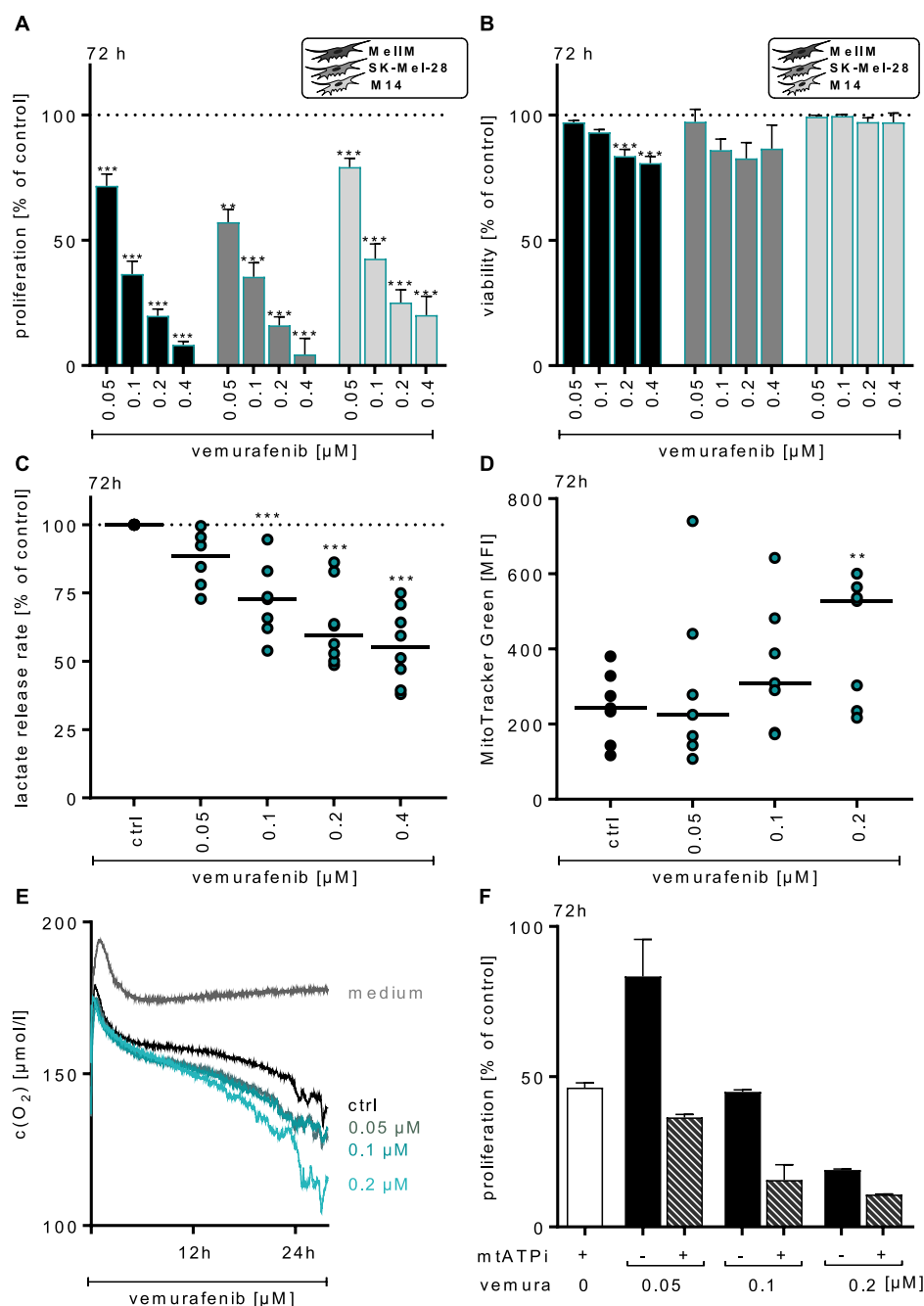


Fig. 3. Impact of vemurafenib on BRAF^{V600E} mutated melanoma cell lines. (A) Proliferation and (B) cell viability of MelIM, SK-Mel-28 and M14 under vemurafenib treatment (0.05–0.4 μM) for 72 h. Proliferation was determined using a CASY cell counter and corrected for the number of cells initially seeded. Results were normalized to control numbers (mean + SEM; n = 14 except n = 12 for 0.05 μM for MelIM; n = 7 except n = 5 for 0.4 μM for SK-Mel-28; n = 8 except n = 6 for 0.4 μM for M14). Cell viability was analyzed by Annexin/7-AAD staining (mean + SEM; n = 10 except for 0.05 μM n = 8 for MelIM; n = 5 for SK-Mel-28; n = 6 for M14). (C) Lactate release rates and (D) mitochondrial content of MelIM cells in the presence or absence of vemurafenib. Lactate levels were measured in cell culture supernatants after 72 h and corrected for basal medium values as well as proliferation. (D) MitoTracker Green staining of MelIM cells incubated in standard growth medium ± vemurafenib for 72 h. Mean fluorescence intensity (MFI) of MitoTracker Green was normalized to unstained cells. (E) Oxygen consumption rates of MelIM cells incubated in standard growth medium ± vemurafenib. Data were acquired by the PreSens technology (mean; n = 3 except for 0.2 μM n = 2). (F) Proliferation of MelIM cells treated with vemurafenib (vemura) in the presence or absence of the ATP synthase inhibitor oligomycin (mtATPi). Results were normalized to controls (mean + SEM, n = 3; one-way ANOVA, post-hoc Dunnett's multiple comparisons test *p < 0.05, **p < 0.01, ***p < 0.001). (For interpretation of the references to color in this figure legend, the reader is referred to the Web version of this article.)

3.4. NSAIDs enhance the anti-metabolic impact of RAF inhibitors

As a metabolic inhibitor vemurafenib can reduce glycolytic activity (Fig. 3). However, its anti-glycolytic impact is not sufficient to completely starve melanoma cells due to remaining basal glycolytic activity on the one hand (Fig. 3C) and compensatory upregulation of OXPHOS on the other hand (Fig. 3D and 3E). In contrast, diclofenac and lumiracoxib are able to metabolically restrict BRAF^{V600E} mutated melanoma cells by targeting both respiration and glycolytic activity (Fig. 2). While the anti-glycolytic impact of vemurafenib is mainly mediated via the HIF1α/C-MYC-axis [18], diclofenac has been discussed to also target glycolytic key players downstream of C-MYC such as the lactate transporter MCT4 [35]. Thus we hypothesized that NSAID treatment might be able to further enhance the anti-metabolic impact of

vemurafenib (Fig. 4A).

To confirm this hypothesis we monitored lactate production of BRAF^{V600E} mutated MelIM cells cultured with vemurafenib in the presence or absence of low-dose (0.05 mM) diclofenac or lumiracoxib (Fig. 4B). In comparison to monotherapy, lactate release rates of the combinatory approaches were significantly lower. Moreover, analysis of oxygen consumption revealed that addition of diclofenac (Fig. 4C) or lumiracoxib (Fig. 4D) counteracts vemurafenib induced metabolic reprogramming towards enhanced OXPHOS. At higher NSAID concentrations (≥ 0.2 mM) respiration was completely blocked (Fig. S4 A + B).

These data indicate that NSAIDs are able to metabolically sensitize BRAF^{V600E} mutated melanoma cells to subsequent vemurafenib therapy and therefore represent promising combinatorial agents.

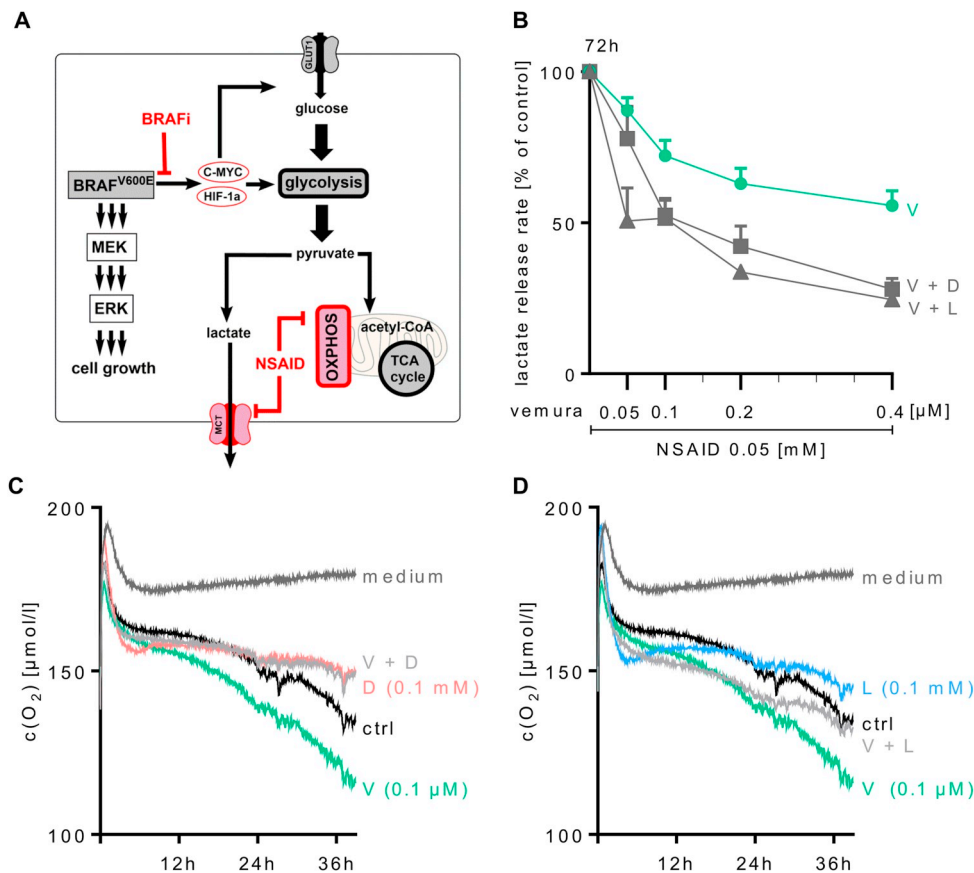


Fig. 4. Impact of the combination of NSAIDs plus vemurafenib on metabolic key features. (A) Schematic model explaining the possible underlying molecular mechanism resulting in the synergism between selected NSAIDs and vemurafenib in BRAF^{V600E} mutated melanoma. (B) Lactate release rates of MeIM cells under single vemurafenib treatment (V; 0.05–0.4 μ M) or in combination with either 0.05 mM diclofenac (V + D) or 0.05 mM lumiracoxib (V + L). Lactate levels were corrected for basal medium values as well as for proliferation kinetics (mean + SEM; n = 3). Oxygen consumption of MeIM cells under vemurafenib treatment in the presence or absence of (C) diclofenac or (D) lumiracoxib (mean; n = 5).

3.5. The combination of vemurafenib and NSAIDs exerts synergistic effects on proliferation arrest and apoptosis induction

To further test whether RAF inhibitors and NSAIDs are synergistic, MeIM (Fig. 5A–D), SK-Mel-28 (Figs. S5A–D) and M14 (Figs. S5E–H) were treated with the combination of vemurafenib (0.05–0.4 μ M) and diclofenac or lumiracoxib (0.05–0.4 mM). Thereby combinatorial concentrations in a fixed constant ratio (1:1000 = [BRAFi]:[NSAID]) according to the IC₅₀ ratio of the single drugs were chosen as previously described [34]. After 72 h proliferation and cell viability were determined and compared to results obtained from single treatment. In all cell lines application of the selected NSAIDs significantly enhanced the impact of BRAFi induced growth inhibition (Fig. 5 A + B, Fig. S5 A + B, Fig. S5 E + F). Especially at moderate concentrations the effect was apparently stronger than the summated impact of the single drugs, assuming synergism. Notably not only proliferation, but also cell viability was affected by combination treatment (Fig. 5 C + D, Fig. S5 C + D, Fig. S5 G + H). While single application of vemurafenib could hardly induce apoptosis, combination therapy with the selected NSAIDs strongly decreased cell viability. This indicates that NSAID treatment potentiates the effect of vemurafenib from cytostatic to cytotoxic.

In order to evaluate drug interactions between vemurafenib and the indicated NSAIDs in more detail, combination indices (CI) for all collected raw data points were calculated (Fig. 5E). CI values represent a mathematical model for the quantification of synergism between two drugs and were generated with CompuSyn according to the method of Chou and Talalay [33]. For vemurafenib plus lumiracoxib all tested combinations were at least additive (0.9 < CI < 1.1) with multiple pockets of moderate to strong synergism (CI < 0.9). Response to vemurafenib plus diclofenac was slightly more heterogeneous among the cell lines with approximately 80% of all tested combinations being synergistic to additive (CI < 1.1).

For further analysis a computerized simulation of synergy

quantification over all three cell lines was performed by median-drug effect plotting (Fig. 5F and G). The model of median drug effect plotting allows to predict the degree of synergism between two drugs for any level of a dose-response curve (fraction affected) calculated from experimentally collected raw data points [33]. Fraction affected (FA) values higher than 0.5 represent an effect greater than 50% of the maximal possible drug effect and are regarded as benchmark for clinically relevant experimental conditions [34]. Calculations of median effect plots averaged over all three cell lines predicted slight to strong synergism for the combination of vemurafenib and diclofenac as well as lumiracoxib. In terms of growth inhibition mean CI values indicate slight synergism for diclofenac (CI_{mean} = 0.90, Fig. 5F) and moderate synergism for lumiracoxib (CI_{mean} = 0.77, Fig. 5G). Cell death inducing effects were regarded as strongly synergistic for both NSAIDs with CI_{mean} values ranging from 0.71 (diclofenac) to 0.46 (lumiracoxib).

These results point out that selective NSAIDs are synergistic with vemurafenib and can efficiently enhance the impact of RAF inhibitor therapy in BRAF^{V600E} mutated melanoma cells from cytostatic to cytotoxic.

3.6. NSAID treatment downregulates MITF expression and delays onset of BRAFi resistance

Nearly all patients suffering from BRAF^{V600E} mutated melanoma acquire resistance to RAF-inhibitors within a few months. Only recently Smith et al. have demonstrated that vemurafenib-induced upregulation of MITF, a key regulator of OXPHOS in melanoma [19], is a major driver of non-mutational drug resistance to RAF inhibitors [36].

The NSAID indomethacin has been shown to reduce MITF transcription in murine melanoma cells [37]. Since we have observed significant inhibition of OXPHOS under NSAID treatment (Fig. 2) and indomethacin reveals structural similarity to the NSAIDs used here, we

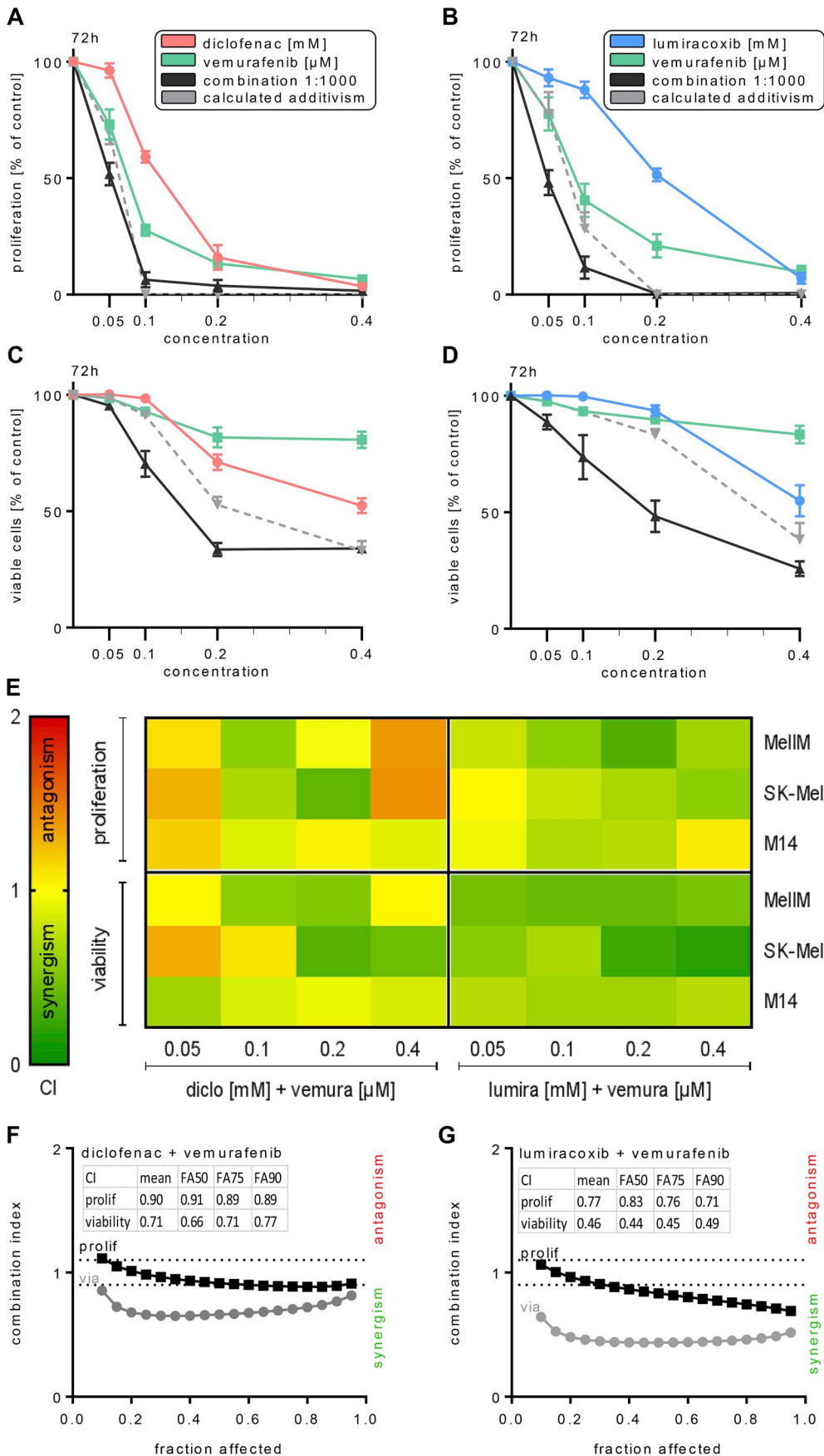


Fig. 5. Synergism of selected NSAIDs and vemurafenib in BRAF^{V600E} mutated melanoma cell lines. (A, B) Proliferation and (C, D) cell viability of MelIM treated with (A, C) diclofenac or (B, D) lumiracoxib (0.05–0.4 mM) and the BRAF-inhibitor vemurafenib (0.05–0.4 μ M) in single use or the combination of both. Dashed curves represent values expected from an additive effect estimated by summation of the single drug impact. Results are given as percentage of untreated controls (mean \pm SEM; n = 5 for diclofenac; n = 6 for lumiracoxib). (E) Heat map of combination indices (CI) showing drug interactions between diclofenac or lumiracoxib and vemurafenib in MelIM, SK-Mel-28 and M14. CI values have been generated with CompuSyn and color-depicted as shown in the legend. Synergistic effects are defined as CI < 0.9 (green), whereas 0.9 < CI < 1.1 indicates additivism (yellow) and CI > 1.1 antagonism (red) of the analyzed drugs. Computerized simulation of drug interactions between vemurafenib and (F) diclofenac or (G) lumiracoxib. Based on raw data obtained from Fig. 4 A–D expected combination indices over different fractions affected (FA; 0.1–0.95) were calculated using CompuSyn. Results represent the mean of all three cell lines (MelIM, SK-Mel-28, M14). Numbers show the mean expected combination indices over all cell lines at clinically relevant fractions affected (FA = 0.5, 0.75, 0.9) as recommended by Bijnsdorp et al. [34]. (For interpretation of the references to color in this figure legend, the reader is referred to the Web version of this article.)

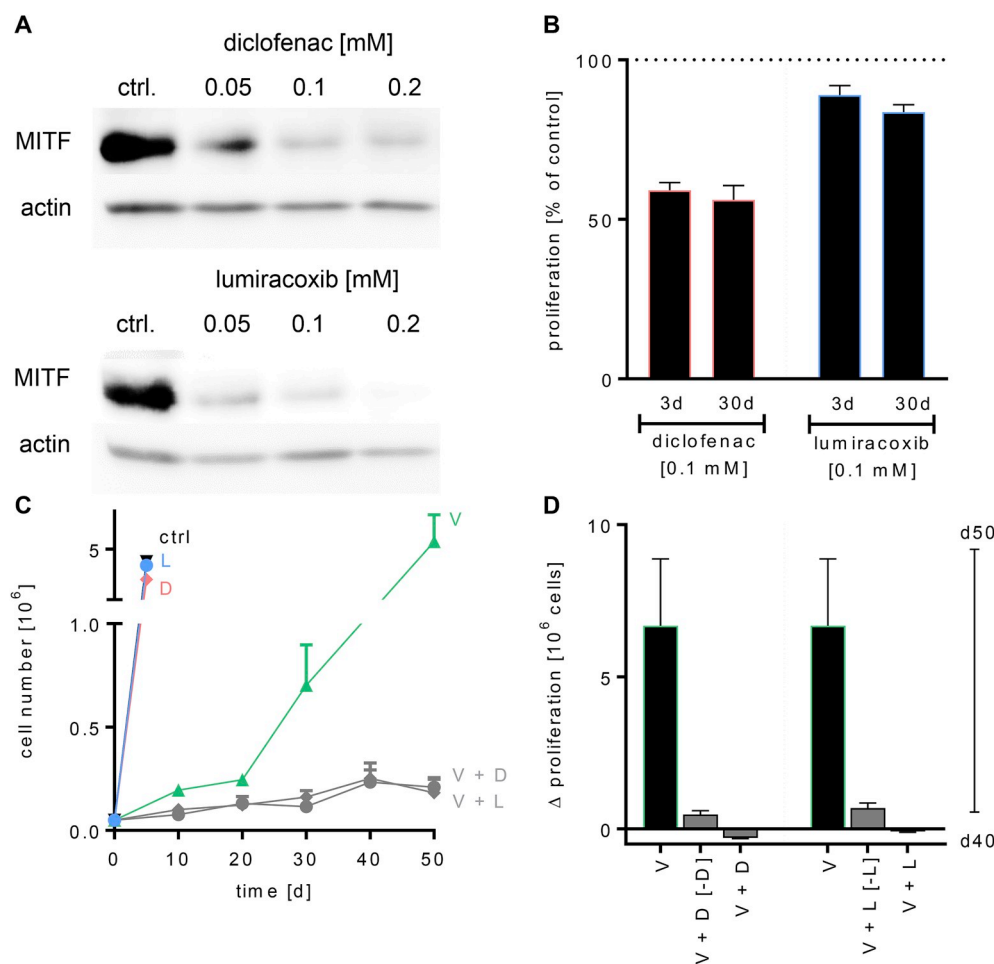


Fig. 6. Impact of long-term NSAID treatment on development of BRAFi-resistance in BRAF^{V600E} mutated melanoma cell lines. (A) Western blot analysis of MITF expression in MelIM. One representative experiment out of two is shown. (B) Proliferation of MelIM cells under diclofenac or lumiracoxib (0.1 mM) for 3 vs. 30 days. Results are given as percentage of untreated controls. (C, D) Proliferation of MelIM cells under long-term vemurafenib ± NSAID therapy. Cells were seeded at low density (0.01×10^6 /ml) and treated with 2.5 μ M vemurafenib (V) in the presence or absence of 0.1 mM diclofenac (D) or lumiracoxib (L) for 50 days. Cells were splitted every 5 days, culture medium and the indicated drugs were refreshed. (D) At day 40 cells treated long-term with vemurafenib and diclofenac (V + D) or lumiracoxib (V + L) were randomized into two subgroups either kept under co-treatment or withdrawn from diclofenac (V + D [-D]) or lumiracoxib (V + L [-L]) for another ten days. Proliferation rates from day 40 to day 50 are shown in comparison to cells under vemurafenib (V) monotherapy (mean + SEM, n = 3).

hypothesized that MITF might be also a target of diclofenac and lumiracoxib. Indeed, western blot analysis of MelIM cells showed downregulation of MITF under both NSAIDs already at low concentrations (0.05 mM) (Fig. 6A). Therefore, diclofenac and lumiracoxib might not only enhance RAF inhibitor therapy by metabolic restriction (Fig. 4), but also delay onset of drug resistance (Fig. S6).

To confirm this hypothesis, proliferation of melanoma cell lines was monitored up to 50 days under high-dose vemurafenib treatment (2.5 μ M) with or without selected NSAIDs (0.1 mM, Fig. 6B–D). Long-term treatment (30 days) of diclofenac (D) or lumiracoxib (L) led to moderate growth inhibition, in fact to the same extent as obtained in short-term analyses (3 days, Fig. 6B). In contrast, cells under RAF inhibitor monotherapy (V) showed initial proliferation arrest, but significant cell regrowth beyond day 20 with doubling times of approximately 2 days indicating gradual loss of drug sensitivity (Fig. 6C and Table 1). Compared to single treatments, cells treated with the combination of vemurafenib and NSAIDs (V + D or V + L) displayed constant proliferation arrest over the whole period of time analyzed (Fig. 6C and Table 1). This suggests that diclofenac and lumiracoxib are able to delay onset of RAF-inhibitor resistance. To clarify this hypothesis, cells co-treated with vemurafenib and NSAIDs were randomized into subgroups at day 40. While part of the cells was further kept under NSAID/vemurafenib co-treatment (V + D or V + L), the other cells were withdrawn from NSAIDs and re-cultivated under vemurafenib monotherapy (V + D[-D] or V + L[-L]) for another 10 days. Notably, those cells removed from NSAID treatment showed no significant regrowth and doubling times were approximately four-fold longer compared to vemurafenib single treatment (Fig. 6D, Table 1). Taken together, these results strongly suggest that addition of diclofenac or lumiracoxib can efficiently delay onset of RAF inhibitor resistance.

4. Discussion

Targeting metabolism has been discussed as a promising therapeutic strategy for melanoma already years ago [8,9]. Up to now, preclinical treatment approaches have mostly focused on either restricting glycolysis [38,39] or OXPHOS [40]. The results of this study, however, provide strong evidence that inhibition of a single energy providing pathway is not sufficient to impair melanoma cells due to their high metabolic flexibility. In a panel of BRAF^{V600E} mutated human melanoma cell lines lack of glucose or mitochondrial inhibition affected

proliferation only up to 50%. Upregulation of mitochondrial content under glucose deprivation confirmed that glycolytic inhibition can be compensated by alternative metabolic pathways. Therefore our data further supports the concept that metabolic plasticity limits the effect of one-armed metabolic therapy approaches what is in line with previously reported studies [27,41]. Since in contrast simultaneous deprivation of glucose and mtATP efficiently starved our cells, we suggest that drugs targeting both glycolysis and OXPHOS are promising candidates for adjuvant melanoma treatment. The idea of combining glycolytic and mitochondrial inhibitors has also been discussed by Chaube et al. lately [42], but was not followed up in patients to date.

With diclofenac and lumiracoxib we have identified two well-known and clinically approved NSAIDs capable to metabolically restrict BRAF^{V600E} mutated melanoma cell lines. Treatment with concentrations as low as 0.05 mM of either NSAID led to a significant reduction of lactate release. The fact that diclofenac can affect glucose metabolism in melanoma cells via downregulation of C-MYC has been shown by our group before [28]. Interestingly, only recently Sasaki et al. have identified the monocarboxylate transporter MCT4 as further target of diclofenac in colon cancer cells [35]. MCTs are known to play a crucial role for maintenance of the highly glycolytic phenotype of BRAF^{V600E} mutated cells as they mediate efflux of lactate into the tumor micro-environment [43] and thereby trigger immune escape [15,44,45]. Hence, MCTs have been considered as a potential target for melanoma therapy already more than a decade ago [46]. Notably Pinheiro et al. have shown that MCT4 is regulated independent from the MAPK pathway [47] whereas MCT1 is a direct downstream target of C-MYC and therefore the BRAF^{V600E} oncogene [18,47]. Thus, the synergistic impact on glycolysis both NSAIDs exerted in combination with vemurafenib might be explained by a simultaneous blockade of C-MYC and MCT4. In accordance with this finding, Abildgaard et al. have shown that the glycolytic inhibitor dichloroacetate can further enhance the metabolic impact of vemurafenib [38].

RAF inhibitors (BRAFi) such as vemurafenib are known to render melanoma addicted to mitochondrial energy supply [21,22]. In single use BRAFi treatment induces strong proliferation arrest, but often no significant cell death. The lack of pro-apoptotic impact is a well-described problem of BRAFi therapy and has been discussed to account for limited treatment efficiency of MAPK inhibitors [30,48,49]. Metabolic flexibility might contribute to this escape from cell death. Accordingly, Trotta et al. showed that disruption of the mitochondrial chain can enhance the pro-apoptotic effect of vemurafenib [23]. Besides restriction of glucose metabolism diclofenac and lumiracoxib have also affected mitochondrial activity in all tested BRAF^{V600E} mutated cell lines. Impairment of OXPHOS could be verified by both downregulated mitochondrial content and oxygen consumption. Several years ago Albano et al. reported mitochondrial dysfunction during diclofenac-induced apoptosis in melanoma [50]. However, the exact mechanism has remained unclear so far. Haq et al. have identified MITF as direct regulator of the mitochondrial master regulator PGC-1 α in BRAF^{V600E} mutated melanoma [19]. As both NSAIDs were capable to reduce MITF expression the selected NSAIDs might restrict OXPHOS via MITF downregulation.

The combination of low concentrations of either NSAID with vemurafenib resulted not only in a more pronounced decrease in proliferation but also in cell death induction. Especially the latter result is interesting as neither vemurafenib monotherapy nor the combination of vemurafenib and oligomycin has been able to induce apoptosis. However, treatment with the mitochondrial ATP synthase inhibitor oligomycin in glucose free medium was able to trigger cell death in melanoma cells. This indicates that blocking metabolic reprogramming towards OXPHOS can enhance the impact of RAF inhibitors on proliferation, but for induction of cell death additional glycolytic restriction as observed under NSAID treatment seems to be crucial.

Counteracting upregulation of OXPHOS is not only capable of enhancing MAPK inhibition [51,52], but has also been discussed as a

promising strategy to overcome drug resistance [25,53,54]. The idea that mitochondrial activity plays a central role in acquisition of resistance followed shortly after FDA approval of vemurafenib [26,55]. By now several groups have shown that vemurafenib-induced upregulation of OXPHOS via MITF is a major driver of non-mutational resistance [36,56–58]. Here we show that administration of diclofenac and lumiracoxib was able to delay vemurafenib resistance. The observed reduction in MITF expression under diclofenac or lumiracoxib treatment might be the underlying mechanistic explanation, but warrants further investigation. Furthermore, Ennen et al. have described a subpopulation of melanoma cells that escape MITF mediated regulation of metabolism by switching towards a MITF_{low} phenotype [59]. Therefore selection of MITF_{low} subclones needs to be taken into consideration as a possible strategy of melanoma to escape from treatment and long-term impact of NSAIDs on such clones should be evaluated.

Several reports indicate that the NSAID concentrations used in this study are physiologically relevant [60,61]. The official prescribing information of diclofenac states plasma levels of 0.15–105 mg/l (~50–350 μ M) to be achievable with recommended doses [62]. Other studies report peak plasma levels (c_{max}) of 12.5 μ M and 20 μ M, respectively, after oral application of single doses diclofenac (50 mg) or lumiracoxib (200 mg) [60,63]. However, c_{max} concentrations are known to increase in a dose-proportional manner and dose escalation towards maximal daily standard doses can further boost reachable plasma concentrations [60,61]. Moreover, intravenous application results in at least two fold higher plasma concentrations compared to oral application [60,64]. About three times higher steady-state levels of both drugs accumulate in synovial fluid [65,66] indicating that similar concentrations could also be reached in tumors.

In conclusion our data provides strong evidence that patients suffering from advanced melanoma, especially those treated with RAF inhibitors, might benefit from adjuvant application of anti-metabolic NSAIDs such as diclofenac and lumiracoxib. Since pain killers are usually included in the therapy of advanced tumors [67], current treatment protocols could easily be adapted.

Disclosure of potential conflicts of interest

There are no conflicts of interest.

Grant support

This study was supported by KFO262, a clinical research unit funded by the Deutsche Forschungsgemeinschaft.

CRediT authorship contribution statement

Christina Brummer: Conceptualization, Data curation, Formal analysis, Writing – review & editing. **Stephanie Faerber:** Data curation. **Christina Bruss:** Data curation. **Christian Blank:** Resources, Writing – review & editing. **Ruben Lacroix:** Data curation. **Sebastian Haferkamp:** Resources, Writing – review & editing. **Wolfgang Herr:** Funding acquisition, Writing – review & editing. **Marina Kreutz:** Conceptualization, Supervision, Project administration, Funding acquisition, Writing – review & editing. **Kathrin Renner:** Conceptualization, Supervision, Project administration, Funding acquisition, Writing – original draft, Writing – review & editing.

Acknowledgement

We acknowledge excellent technical assistance of Gabriele Schoenhammer and Monika Wehrstein.

Appendix A. Supplementary data

Supplementary data to this article can be found online at <https://doi.org/10.1016/j.canlet.2018.11.018>.

References

- [1] P.B. Chapman, A. Hauschild, C. Robert, J.B. Haanen, P. Ascierto, J. Larkin, R. Dummer, C. Garbe, A. Testori, M. Maio, D. Hogg, P. Lorigan, C. Lebbe, T. Jouary, D. Schadendorf, A. Ribas, S.J. O'Day, J.A. Sosman, J.M. Kirkwood, A.M.M. Eggermont, B. Dreno, K. Nolop, J. Li, B. Nelson, J. Hou, R.J. Lee, K.T. Flaherty, G.A. McArthur, BRIM-3 Study Group, Improved survival with vemurafenib in melanoma with BRAF V600E mutation, *N. Engl. J. Med.* 364 (2011) 2507–2516, <https://doi.org/10.1056/NEJMoa1103782>.
- [2] H. Davies, G.R. Bignell, C. Cox, P. Stephens, S. Edkins, S. Clegg, J. Teague, H. Woffendin, M.J. Garnett, W. Bottomley, N. Davis, E. Dicks, R. Ewing, Y. Floyd, K. Gray, S. Hall, R. Hawes, J. Hughes, V. Kosmidou, A. Menzies, C. Mould, A. Parker, C. Stevens, S. Watt, S. Hooper, R. Wilson, H. Jayatilake, B.A. Gusterson, C. Cooper, J. Shipley, D. Hargrave, K. Pritchard-Jones, N. Maitland, G. Chenevix-Trench, G.J. Riggins, D.D. Bigner, G. Palmieri, A. Cossu, A. Flanagan, A. Nicholson, J.W.C. Ho, S.Y. Leung, S.T. Yuen, B.L. Weber, H.F. Seigler, T.L. Darrow, H. Paterson, R. Marais, C.J. Marshall, R. Wooster, M.R. Stratton, P.A. Futreal, Mutations of the BRAF gene in human cancer, *Nature* 417 (2002) 949–954, <https://doi.org/10.1038/nature00766>.
- [3] J.A. Sosman, K.B. Kim, L. Schuchter, R. Gonzalez, A.C. Pavlick, J.S. Weber, G.A. McArthur, T.E. Hutson, S.J. Moschos, K.T. Flaherty, P. Hersey, R. Kefford, D. Lawrence, I. Puzanov, K.D. Lewis, R.K. Amaravadi, B. Chmielowski, H.J. Lawrence, Y. Shyr, F. Ye, J. Li, K.B. Nolop, R.J. Lee, A.K. Joe, A. Ribas, Survival in BRAF V600-mutant advanced melanoma treated with vemurafenib, *N. Engl. J. Med.* 366 (2012) 707–714, <https://doi.org/10.1056/NEJMoa1112302>.
- [4] J.J. Luke, K.T. Flaherty, A. Ribas, G.V. Long, Targeted agents and immunotherapies: optimizing outcomes in melanoma, *Nat. Rev. Clin. Oncol.* 14 (2017) 463–482, <https://doi.org/10.1038/nrclinonc.2017.43>.
- [5] E. Simeone, A.M. Grimaldi, L. Festino, V. Vanella, M. Palla, P.A. Ascierto, Combination treatment of patients with BRAF-mutant melanoma: a new standard of care, *BioDrugs Clin. Immunother. Biopharm. Gene Ther.* 31 (2017) 51–61, <https://doi.org/10.1007/s40259-016-0208-z>.
- [6] G.V. Long, Z. Eroglu, J. Infante, S. Patel, A. Daud, D.B. Johnson, R. Gonzalez, R. Kefford, O. Hamid, L. Schuchter, J. Cebon, W. Sharfman, R. McWilliams, M. Sznol, S. Redhu, E. Gasal, B. Mookerjee, J. Weber, K.T. Flaherty, Long-term outcomes in patients with BRAF V600-mutant metastatic melanoma who received dabrafenib combined with trametinib, *J. Clin. Oncol.* 36 (2018) 667–673, <https://doi.org/10.1200/JCO.2017.74.1025>.
- [7] D. Schadendorf, G.V. Long, D. Stroiakovski, B. Karaszewska, A. Hauschild, E. Levchenko, V. Chiarion-Sileni, J. Schachter, C. Garbe, C. Dutriaux, H. Gogas, M. Mandalà, J.B.A.G. Haanen, C. Lebbe, A. Mackiewicz, P. Rutkowski, J.-J. Grob, P. Nathan, A. Ribas, M.A. Davies, Y. Zhang, M. Kaper, B. Mookerjee, J.J. Legos, K.T. Flaherty, C. Robert, Three-year pooled analysis of factors associated with clinical outcomes across dabrafenib and trametinib combination therapy phase 3 randomised trials, *Eur. J. Canc.* 82 (2017) 45–55, <https://doi.org/10.1016/j.ejca.2017.05.033>.
- [8] L.K. Smith, A.D. Rao, G.A. McArthur, Targeting metabolic reprogramming as a potential therapeutic strategy in melanoma, *Pharmacol. Res.* (2016), <https://doi.org/10.1016/j.phrs.2016.02.009>.
- [9] G.M. Fischer, Y.N. Vashisht Gopal, J.L. McQuade, W. Peng, R.J. DeBerardinis, M.A. Davies, Metabolic strategies of melanoma cells: mechanisms, interactions with the tumor microenvironment, and therapeutic implications, *Pigment Cell Melanoma Res* (2017), <https://doi.org/10.1111/pcmr.12661>.
- [10] M. Hosseini, Z. Kasraian, H.R. Rezvani, Energy metabolism in skin cancers: a therapeutic perspective, *Biochim. Biophys. Acta BBA - Bioenerg.* 1858 (2017) 712–722, <https://doi.org/10.1016/j.bbabi.2017.01.013>.
- [11] O. Warburg, On the origin of cancer cells, *Science* 123 (1956) 309–314, <https://doi.org/10.1126/science.123.3191.309>.
- [12] D. Hanahan, R.A. Weinberg, Hallmarks of cancer: the next generation, *Cell* 144 (2011) 646–674, <https://doi.org/10.1016/j.cell.2011.02.013>.
- [13] D.A. Scott, A.D. Richardson, F.V. Filipp, C.A. Knutzen, G.G. Chiang, Z.A. Ronai, A.L. Osterman, J.W. Smith, Comparative metabolic flux profiling of melanoma cell lines: BEYOND the WARBURG effect, *J. Biol. Chem.* 286 (2011) 42626–42634, <https://doi.org/10.1074/jbc.M111.282046>.
- [14] I.J. Bettum, S.S. Gorad, A. Barkovskaya, S. Pettersen, S.A. Moestue, K. Vasiliauskaitė, E. Tenstad, T. Øyjord, Ø. Risa, V. Nygaard, G.M. Mølandsmo, L. Prasmackaitė, Metabolic reprogramming supports the invasive phenotype in malignant melanoma, *Cancer Lett.* 366 (2015) 71–83, <https://doi.org/10.1016/j.canlet.2015.06.006>.
- [15] A. Brand, K. Singer, G.E. Koehl, M. Kolitzus, G. Schoenhammer, A. Thiel, C. Matos, C. Bruss, S. Klobuch, K. Peter, M. Kastenberger, C. Bogdan, U. Schleicher, A. Mackensen, E. Ullrich, S. Fichtner-Feigl, R. Kesselring, M. Mack, U. Ritter, M. Schmid, C. Blank, K. Dettmer, P.J. Oefner, P. Hoffmann, S. Walenta, E.K. Geissler, J. Pouyssegur, A. Villunger, A. Steven, B. Seliger, S. Schreml, S. Haferkamp, E. Kohl, S. Karrer, M. Berneburg, W. Herr, W. Mueller-Klieser, K. Renner, M. Kreutz, LDHA-associated lactic acid production blunts tumor immunosurveillance by T and NK cells, *Cell Metabol.* 24 (2016) 657–671, <https://doi.org/10.1016/j.cmet.2016.08.011>.
- [16] C. Abildgaard, P. Guldborg, Molecular drivers of cellular metabolic reprogramming in melanoma, *Trends Mol. Med.* 21 (2015) 164–171, <https://doi.org/10.1016/j.molmed.2014.12.007>.
- [17] A. Hall, K.D. Meyle, M.K. Lange, M. Klima, M. Sanderhoff, C. Dahl, C. Abildgaard, K. Thorup, S.M. Moghimi, P.B. Jensen, J. Bartek, P. Guldborg, C. Christensen, Dysfunctional oxidative phosphorylation makes malignant melanoma cells addicted to glycolysis driven by the (V600E)BRAF oncogene, *Oncotarget* 4 (2013) 584–599.
- [18] T.J. Parmenter, M. Kleinschmidt, K.M. Kinross, S.T. Bond, J. Li, M.R. Kaadige, A. Rao, K.E. Sheppard, W. Hugo, G.M. Pupo, R.B. Pearson, S.L. McGee, G.V. Long, R.A. Scolyer, H. Rizos, R.S. Lo, C. Cullinane, D.E. Ayer, A. Ribas, R.W. Johnstone, R.J. Hicks, G.A. McArthur, Response of BRAF-mutant melanoma to BRAF inhibition is mediated by a network of transcriptional regulators of glycolysis, *Cancer Discov.* 4 (2014) 423–433, <https://doi.org/10.1158/2159-8290.CD-13-0440>.
- [19] R. Haq, J. Shoaq, P. Andreu-Perez, S. Yokoyama, H. Edelman, G.C. Rowe, D.T. Frederick, A.D. Hurley, A. Nellore, A.L. Kung, J.A. Wargo, J.S. Song, D.E. Fisher, Z. Arany, H.R. Widlund, Oncogenic BRAF regulates oxidative metabolism via PGC1 α and MITF, *Cancer Cell* 23 (2013) 302–315, <https://doi.org/10.1016/j.ccr.2013.02.003>.
- [20] R. Haq, D.E. Fisher, H.R. Widlund, Molecular pathways: BRAF induces bioenergetic adaptation by attenuating oxidative phosphorylation, *Clin. Canc. Res.* 20 (2014) 2257–2263, <https://doi.org/10.1158/1078-0432.CCR-13-0898>.
- [21] N. Theodosakis, M.A. Held, A. Marzuka-Alcala, K.M. Meeth, G. Micevic, G.V. Long, R.A. Scolyer, D.F. Stern, M.W. Bosenberg, BRAF inhibition decreases cellular glucose uptake in melanoma in association with reduction in cell volume, *Mol. Canc. Therapeut.* 14 (2015) 1680–1692, <https://doi.org/10.1158/1535-7163.MCT-15-0080>.
- [22] T. Delgado-Goni, M.F. Miniotti, S. Wantuch, H.G. Parkes, R. Marais, P. Workman, M.O. Leach, M. Belouche-Babari, The BRAF inhibitor vemurafenib activates mitochondrial metabolism and inhibits hyperpolarized pyruvate-lactate exchange in BRAF-mutant human melanoma cells, *Mol. Canc. Therapeut.* 15 (2016) 2987–2999, <https://doi.org/10.1158/1535-7163.MCT-16-0068>.
- [23] A.P. Trotta, J.D. Gelles, M.N. Serasinghe, P. Loi, J.L. Arbiser, J.E. Chipuk, Disruption of mitochondrial electron transport chain function potentiates the proapoptotic effects of MAPK inhibition, *J. Biol. Chem.* 292 (2017) 11727–11739, <https://doi.org/10.1074/jbc.M117.786442>.
- [24] P. Marchetti, A. Trinh, R. Khamari, J. Kluzza, Melanoma metabolism contributes to the cellular responses to MAPK/ERK pathway inhibitors, *Biochim. Biophys. Acta BBA - Gen. Subj.* 1862 (2018) 999–1005, <https://doi.org/10.1016/j.bbagen.2018.01.018>.
- [25] E. Livingstone, S. Swann, C. Lilla, D. Schadendorf, A. Roesch, Combining BRAF(V) (600E) inhibition with modulators of the mitochondrial bioenergetic metabolism to overcome drug resistance in metastatic melanoma, *Exp. Dermatol.* (2015), <https://doi.org/10.1111/exd.12718>.
- [26] P. Corazao-Rozas, P. Guerreschi, M. Jendoubi, F. André, A. Jonneaux, C. Scalbert, G. Garçon, M. Malet-Martino, S. Balayssac, S. Rocchi, A. Savina, P. Formstecher, L. Mortier, J. Kluzza, P. Marchetti, Mitochondrial oxidative stress is the Achilles' heel of melanoma cells resistant to BRAF-mutant inhibitor, *Oncotarget* 4 (2013) 1986–1998.
- [27] J.-H. Lim, C. Luo, F. Vazquez, P. Puigserver, Targeting mitochondrial oxidative metabolism in melanoma causes metabolic compensation through glucose and glutamine utilization, *Cancer Res.* 74 (2014) 3535–3545, <https://doi.org/10.1158/0008-5472.CAN-13-2893-T>.
- [28] E. Gottfried, S.A. Lang, K. Renner, A. Bosserhoff, W. Gronwald, M. Rehli, S. Einhell, I. Gedig, K. Singer, A. Seilbeck, A. Mackensen, O. Grauer, P. Hau, K. Dettmer, R. Andreesen, P.J. Oefner, M. Kreutz, New Aspects of an Old Drug – diclofenac Targets MYC and glucose metabolism in tumor cells, *PLoS One* 8 (2013) e66987, <https://doi.org/10.1371/journal.pone.0066987>.
- [29] K. Jacob, A.K. Bosserhoff, F. Wach, R. Knüchel, E.C. Klein, R. Hein, R. Buettner, Characterization of selected strongly and weakly invasive sublines of a primary human melanoma cell line and isolation of subtractive cDNA clones, *Int. J. Canc.* 60 (1995) 668–675.
- [30] S. Haferkamp, A. Borst, C. Adam, T.M. Becker, S. Motschenbacher, S. Windhövel, A.L. Hufnagel, R. Houben, S. Meierjohann, Vemurafenib induces senescence features in melanoma cells, *J. Invest. Dermatol.* 133 (2013) 1601–1609, <https://doi.org/10.1038/jid.2013.6>.
- [31] V. Roth, Doubling Time Computing, (2006) Roth V. 2006 Doubling Time Computing, Available from: <http://www.doubling-time.com/compute.php>.
- [32] M. Jain, R. Nilsson, S. Sharma, N. Madhusudhan, T. Kitami, A.L. Souza, R. Kafri, M. Kirschner, C.B. Clish, V.K. Mootha, Metabolite profiling identifies a key role for glycine in rapid cancer cell proliferation, *Science* 336 (2012) 1040–1044, <https://doi.org/10.1126/science.1218595>.
- [33] T.-C. Chou, Drug combination studies and their synergy quantification using the Chou-Talalay method, *Cancer Res.* 70 (2010) 440–446, <https://doi.org/10.1158/0008-5472.CAN-09-1947>.
- [34] I.V. Bijsdorp, E. Giovannetti, G.J. Peters, Analysis of drug interactions, *Methods Mol. Biol. Clifton NJ* 731 (2011) 421–434, https://doi.org/10.1007/978-1-61779-080-5_34.
- [35] S. Sasaki, Y. Futagi, M. Ideno, M. Kobayashi, K. Narumi, A. Furugen, K. Iseki, Effect of diclofenac on SLC16A3/MCT4 by the Caco-2 cell line, *Drug Metabol. Pharmacokin.* 31 (2016) 218–223, <https://doi.org/10.1016/j.dmpk.2016.03.004>.
- [36] M.P. Smith, H. Brunton, E.J. Rowling, J. Ferguson, I. Arozarena, Z. Miskolczi, J.L. Lee, M.R. Girotti, R. Marais, M.P. Levesque, R. Dummer, D.T. Frederick, K.T. Flaherty, Z.A. Cooper, J.A. Wargo, C. Wellbrock, Inhibiting drivers of non-mutational drug tolerance is a salvage strategy for targeted melanoma therapy, *Cancer Cell* 29 (2016) 270–284, <https://doi.org/10.1016/j.ccell.2016.02.003>.
- [37] K. Sato, M. Takei, R. Iyota, Y. Muraoka, M. Nagashima, Y. Yoshimura, Indomethacin inhibits melanogenesis via down-regulation of Mitf mRNA transcription, *Biosci.*

- Biotechnol. Biochem. 81 (2017) 2307–2313, <https://doi.org/10.1080/09168451.2017.1394812>.
- [38] C. Abildgaard, C. Dahl, A.L. Basse, T. Ma, P. Guldborg, Bioenergetic modulation with dichloroacetate reduces the growth of melanoma cells and potentiates their response to BRAFV600E inhibition, *J. Transl. Med.* 12 (2014) 247, <https://doi.org/10.1186/s12967-014-0247-5>.
- [39] J.-Z. Qin, H. Xin, B.J. Nickoloff, 2-Deoxyglucose sensitizes melanoma cells to TRAIL-induced apoptosis which is reduced by mannose, *Biochem. Biophys. Res. Commun.* 401 (2010) 293–299, <https://doi.org/10.1016/j.bbrc.2010.09.054>.
- [40] T.M. Ashton, W.G. McKenna, L.A. Kunz-Schughart, G.S. Higgins, Oxidative phosphorylation as an emerging target in cancer therapy, *Clin. Cancer Res. Off. J. Am. Assoc. Cancer Res.* (2018), <https://doi.org/10.1158/1078-0432.CCR-17-3070>.
- [41] J. Kluza, P. Corazao-Rozas, Y. Touil, M. Jendoubi, C. Maire, P. Guerreschi, A. Jonneaux, C. Ballot, S. Balayssac, S. Valable, A. Corroyer-Dulmont, M. Bernaudin, M. Malet-Martino, E.M. de Lassalle, P. Maboudou, P. Formstecher, R. Polakowska, L. Mortier, P. Marchetti, Inactivation of the HIF-1/PDK3 signaling Axis drives melanoma toward mitochondrial oxidative metabolism and potentiates the therapeutic activity of pro-oxidants, *Cancer Res.* 72 (2012) 5035–5047, <https://doi.org/10.1158/0008-5472.CAN-12-0979>.
- [42] B. Chaube, P. Malvi, S.V. Singh, N. Mohammad, A.S. Meena, M.K. Bhat, Targeting metabolic flexibility by simultaneously inhibiting respiratory complex I and lactate generation retards melanoma progression, *Oncotarget* 6 (2015) 37281–37299, <https://doi.org/10.18632/oncotarget.6134>.
- [43] C. Pinheiro, A. Longatto-Filho, J. Azevedo-Silva, M. Casal, F.C. Schmitt, F. Baltazar, Role of monocarboxylate transporters in human cancers: state of the art, *J. Bioenerg. Biomembr.* 44 (2012) 127–139, <https://doi.org/10.1007/s10863-012-9428-1>.
- [44] I. Böhme, A.K. Bosserhoff, Acidic tumor microenvironment in human melanoma, *Pigment Cell Melanoma Res* 29 (2016) 508–523, <https://doi.org/10.1111/pcmr.12495>.
- [45] I. Marchiq, J. Pouyssegur, Hypoxia, cancer metabolism and the therapeutic benefit of targeting lactate/H(+) symporters, *J. Mol. Med. Berl. Ger.* 94 (2016) 155–171, <https://doi.org/10.1007/s00109-015-1307-x>.
- [46] M.L. Wahl, J.A. Owen, R. Burd, R.A. Herlands, S.S. Nogami, U. Rodeck, D. Bernd, D.B. Leeper, C.S. Owen, Regulation of intracellular pH in human melanoma: potential therapeutic implications, *Mol. Canc. Therapeut.* 1 (2002) 617–628.
- [47] C. Pinheiro, V. Miranda-Gonçalves, A. Longatto-Filho, A.L.S.A. Vicente, G.N. Berardinelli, C. Scapulatempo-Neto, R.F.A. Costa, C.R. Viana, R.M. Reis, F. Baltazar, V.L. Vazquez, The metabolic microenvironment of melanomas: prognostic value of MCT1 and MCT4, *Cell Cycle* 15 (2016) 1462–1470, <https://doi.org/10.1080/15384101.2016.1175258>.
- [48] R. Haq, S. Yokoyama, E.B. Hawryluk, G.B. Jönsson, D.T. Frederick, K. McHenry, D. Porter, T.-N. Tran, K.T. Love, R. Langer, D.G. Anderson, L.A. Garraway, L.M. Duncan, D.L. Morton, D.S.B. Hoon, J.A. Wargo, J.S. Song, D.E. Fisher, BCL2L1 is a lineage-specific antiapoptotic melanoma oncogene that confers resistance to BRAF inhibition, *Proc. Natl. Acad. Sci. U. S. A* 110 (2013) 4321–4326, <https://doi.org/10.1073/pnas.1205575110>.
- [49] M.N. Serasinghe, D.J. Missert, J.J. Ascioia, S. Podgrabska, S.Y. Wieder, S. Izadmehr, G. Belbin, M. Skobe, J.E. Chipuk, Anti-apoptotic BCL-2 proteins govern cellular outcome following B-RAF(V600E) inhibition and can be targeted to reduce resistance, *Oncogene* 34 (2015) 857–867, <https://doi.org/10.1038/onc.2014.21>.
- [50] F. Albano, A. Arcucci, G. Granato, S. Romano, S. Montagnani, E. De Vendittis, M.R. Ruocco, Markers of mitochondrial dysfunction during the diclofenac-induced apoptosis in melanoma cell lines, *Biochimie* 95 (2013) 934–945, <https://doi.org/10.1016/j.biochi.2012.12.012>.
- [51] S. Aida, Y. Sonobe, H. Tanimura, N. Oikawa, M. Yuhki, H. Sakamoto, T. Mizuno, MITF suppression improves the sensitivity of melanoma cells to a BRAF inhibitor, *Cancer Lett.* 409 (2017) 116–124, <https://doi.org/10.1016/j.canlet.2017.09.008>.
- [52] K. Kido, H. Sumimoto, S. Asada, S.M. Okada, T. Yaguchi, N. Kawamura, M. Miyagishi, T. Saida, Y. Kawakami, Simultaneous suppression of MITF and BRAF^{V600E} enhanced inhibition of melanoma cell proliferation, *Cancer Sci.* 100 (2009) 1863–1869, <https://doi.org/10.1111/j.1349-7006.2009.01266.x>.
- [53] J.L. McQuade, Y. Vashisht Gopal, Counteracting oxidative phosphorylation-mediated resistance of melanomas to MAPK pathway inhibition, *Mol. Cell. Oncol.* 2 (2015) e991610, <https://doi.org/10.4161/23723556.2014.991610>.
- [54] F. Baenke, B. Chaneton, M. Smith, N. Van Den Broek, K. Hogan, H. Tang, A. Viros, M. Martin, L. Galbraith, M.R. Girotti, N. Dhomen, E. Gottlieb, R. Marais, Resistance to BRAF inhibitors induces glutamine dependency in melanoma cells, *Mol. Oncol.* 10 (2016) 73–84, <https://doi.org/10.1016/j.molonc.2015.08.003>.
- [55] M. Cierlitz, H. Chauvistré, I. Bogeski, X. Zhang, A. Hauschild, M. Herlyn, D. Schadendorf, T. Vogt, A. Roesch, Mitochondrial oxidative stress as a novel therapeutic target to overcome intrinsic drug resistance in melanoma cell subpopulations, *Exp. Dermatol.* (2014), <https://doi.org/10.1111/exd.12613> n/a-n/a.
- [56] C.M. Johannessen, L.A. Johnson, F. Piccioni, A. Townes, D.T. Frederick, M.K. Donahue, R. Narayan, K.T. Flaherty, J.A. Wargo, D.E. Root, L.A. Garraway, A melanocyte lineage program confers resistance to MAP kinase pathway inhibition, *Nature* 504 (2013) 138–142, <https://doi.org/10.1038/nature12688>.
- [57] I. Arozarena, M.P. Smith, C. Wellbrock, Targeting MITF in the tolerance-phase, *Oncotarget* 7 (2016) 54094–54095, <https://doi.org/10.18632/oncotarget.9423>.
- [58] M.P. Smith, C. Wellbrock, Molecular pathways: maintaining MAPK inhibitor sensitivity by targeting nonmutational tolerance, *Clin. Cancer Res. Off. J. Am. Assoc. Cancer Res.* 22 (2016) 5966–5970, <https://doi.org/10.1158/1078-0432.CCR-16-0954>.
- [59] M. Ennen, C. Keime, G. Gambi, A. Kieny, S. Coassolo, C. Thibault-Carpentier, F. Margerin-Schaller, G. Davidson, C. Vagne, D. Lipsker, I. Davidson, MITF-high and MITF-low cells and a novel subpopulation expressing genes of both cell states contribute to intra- and intertumoral heterogeneity of primary melanoma, *Clin. Cancer Res. Off. J. Am. Assoc. Cancer Res.* 23 (2017) 7097–7107, <https://doi.org/10.1158/1078-0432.CCR-17-0010>.
- [60] C.M. Rordorf, L. Choi, P. Marshall, J.B. Mangold, Clinical pharmacology of lumiracoxib: a selective cyclo-oxygenase-2 inhibitor, *Clin. Pharmacokinet.* 44 (2005) 1247–1266, <https://doi.org/10.2165/00003088-200544120-00004>.
- [61] N.M. Davies, K.E. Anderson, Clinical pharmacokinetics of diclofenac: therapeutic insights and pitfalls, *Clin. Pharmacokinet.* 33 (1997) 184–213, <https://doi.org/10.2165/00003088-199733030-00003>.
- [62] FDA, Prescribing Information “diclofenac Sodium Enteric-coated Tablets, (2018) https://www.accessdata.fda.gov/drugsatfda_docs/label/2009/019201s0381bl.pdf, Accessed date: 26 October 2018.
- [63] B. Mukherjee, S. Mahapatra, S. Das, G. Roy, S. Dey, HPLC detection of plasma concentrations of diclofenac in human volunteers administered with povidone-ethylcellulose-based experimental transdermal matrix-type patches, *Meth. Find. Exp. Clin. Pharmacol.* 28 (2006) 301–306, <https://doi.org/10.1358/mf.2006.28.5.1000338>.
- [64] J.V. Willis, M.J. Kendall, R.M. Flinn, D.P. Thornhill, P.G. Welling, The pharmacokinetics of diclofenac sodium following intravenous and oral administration, *Eur. J. Clin. Pharmacol.* 16 (1979) 405–410, <https://doi.org/10.1007/BF00568201>.
- [65] P.D. Fowler, M.F. Shadforth, P.R. Crook, V.A. John, Plasma and synovial fluid concentrations of diclofenac sodium and its major hydroxylated metabolites during long-term treatment of rheumatoid arthritis, *Eur. J. Clin. Pharmacol.* 25 (1983) 389–394.
- [66] G. Scott, C. Rordorf, C. Reynolds, J. Kalbag, M. Looby, S. Milosavljev, M. Weaver, J.P. Huff, D.A. Ruff, Pharmacokinetics of lumiracoxib in plasma and synovial fluid, *Clin. Pharmacokinet.* 43 (2004) 467–478, <https://doi.org/10.2165/00003088-200443070-00003>.
- [67] S. Mercadante, The use of anti-inflammatory drugs in cancer pain, *Cancer Treat Rev.* 27 (2001) 51–61, <https://doi.org/10.1053/ctrv.2000.0192>.